ELSEVIER

Signal Processing 80 (2000) 1515–1533

SIGNAL PROCESSING

www.elsevier.nl/locate/sigpro

Processing arbitrary-length signals with linear-phase cosine-modulated filter banks

Jörg Kliewer[a,*], Tanja Karp[b], Alfred Mertins[c]

[a]*University of Kiel, Institute for Circuits and Systems Theory, Kaiserstr. 2, 24143 Kiel, Germany*
[b]*University of Mannheim, B6/26, 68131 Mannheim, Germany*
[c]*University of Wollongong, School of Electrical, Computer and Telecomm. Engineering, Wollongong, NSW 2522, Australia*

Received 26 April 1999; received in revised form 21 December 1999

Abstract

This paper presents methods for the decomposition of arbitrary-length signals with linear-phase cosine-modulated filter banks. The analysis filters of this filter bank are divided into two sets having different centers of symmetry. This prohibits the use of standard extension methods as described in the literature. Nevertheless, we show that symmetric extension can be adapted in such a way that the filter bank is support-preservative. Methods for dealing with arbitrary length of both signals and filters are presented. Finally, applications in image and audio coding are outlined. In audio coding the proposed processing methods allow to efficiently avoid pre-echoes.

Zusammenfassung

In diesem Artikel werden Methoden für die Verarbeitung endlich langer Signale mit einer linearphasigen cosinusmodulierten Filterbank vorgestellt. Die Impulsantworten der Analysefilter dieser Filterbank sind in zwei Gruppen mit unterschiedlichen Symmetriezentren aufgeteilt, weshalb herkömmliche Randbehandlungsmethoden aus der Literatur nicht angewendet werden können. Wir stellen eine Modifikation der symmetrischen Reflexion für diese Filterbank vor, die kritische Abtastung auch für endlich lange Signale erlaubt. Dabei darf die Länge des Eingangssignals und der Teilbandfilter–Impulsantworten beliebig sein. Schließlich werden Anwendungen im Bereich der Kompression von Bild- und Audiosignalen vorgestellt. Bei der Audiocodierung erlauben die vorgestellten Randbehandlungsmethoden eine effiziente Unterdrückung von Vorechos.

Résumé

Cet article présente de nouvelles méthodes pour la décomposition de signaux d'une longueur quelconque à l'aide de bancs de filtres modulés en cosinus à phase linéaire. Les filtres d'analyse de ces bancs de filtres se repartissent en deux catégories, ayant des centres de symétrie différents, et ceci interdit l'utilisation de méthodes d'extension classiques que l'on peut trouver dans la littérature. Ici, nous montrons néanmoins qu'il est possible d'adapter la méthode d'extension symétrique pour permettre un sous-échantillonnage critique des signaux de longueur finie, et ce, quelle que soit la longueur des signaux et des filtres. Finalement, des applications en codage d'images et et de signaux audiofréquence sont

* Corresponding author. Tel.: + 49-431-77572-406; fax: + 49-431-77572-403.
E-mail address: jkl@techfak.uni-kiel.de (J. Kliewer)

0165-1684/00/$ - see front matter
PII: S0165-1684(00)00053-0

explicitées. Pour le codage audio, il faut souligner que les traitements proposés permettent de réduire considérablement le phénomène de pré-écho.

Keywords: Symmetric extension; Cosine-modulated filter bank; Arbitrary-length signals; Image coding; Audio coding

1. Introduction

Critically subsampled filter banks are widely used for subband-based coding of speech, audio, images and video. On the analysis side, the input signal is divided into a number of subband signals by means of FIR analysis filters. The subband signals are critically subsampled and then quantized in order to be transmitted or stored. On the synthesis side, the subband signals are first upsampled and then applied to the synthesis filters. The total number of subband samples per time interval is equal to the number of input samples in the same interval. However, when processing finite-length signals, such as the rows and columns of an image, the total number of subband samples is generally larger than the length of the input signal. Thus, the filter bank cannot be regarded as support-preservative in this case. One solution to this problem, which is applicable if the number of input values is an integer multiple of the number of channels, is a periodic extension of the input signal as depicted in Fig. 1(a) [25]. The subband signals are then periodic as well and can be restricted to one period, which finally leads to critical subsampling again. However, this method has the disadvantage that, due to possibly different amplitudes at its borders, the periodically extended signal may show extreme discontinuities that have not been part of the original input signal (see Fig. 1(a)). These discontinuities may lead to additional border distortions when subband quantization is present.

For filter banks with *linear-phase* analysis and synthesis filters, support preservation can also be obtained by a symmetric extension of the input signal at both boundaries (see Fig. 1(b)), provided that all filters have the same center of symmetry [1,22]. The use of symmetric extension methods guarantees – in contrast to a periodic extension of the input signal – a "smooth" behavior at the signal boundaries and thus reduces the border distortions under subband quantization.

Other methods discussed in the literature are based on the design of special boundary filters [5,16], resulting in implementations where the filter coefficients must be switched at the boundaries. Furthermore, time-varying filter banks have been proposed [12,16,20]. Generally, if the boundary filters are obtained by some kind of optimization, a model of the statistical properties of the – in general non-stationary – input signal is needed.

In this paper, we discuss a special class of cosine-modulated filter banks with linear-phase analysis and synthesis filters. Such a system was first presented in [13]. An extension to arbitrary prototype lengths was independently reported in [3,4]. The filter bank can also be regarded as a special case of the modified DFT filter bank [8]. This system has the advantage that due to its modulated nature, the filter bank can be

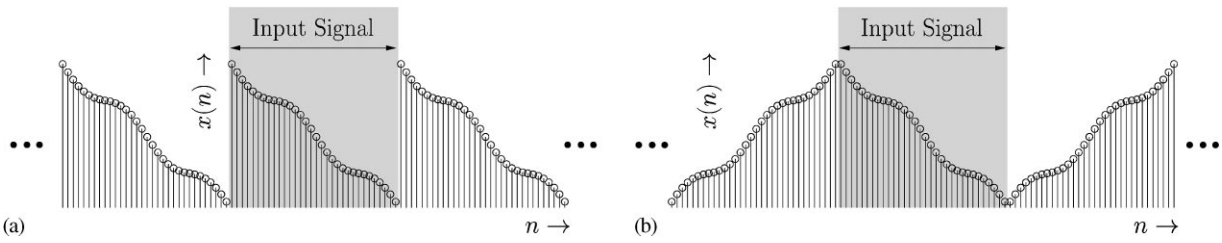

Fig. 1. (a) Periodic and (b) (even) symmetric extension of the input signal.

efficiently realized in a polyphase structure [2,24]. Moreover, compared to general linear-phase filter banks [18,23], the design cost is also reduced. The only drawback is that the linear-phase analysis filters do not have the same center of symmetry. Therefore, standard symmetric extension methods as described in [1,22] cannot be applied to this filter bank. In this paper we propose modified symmetric extension methods for the linear-phase cosine-modulated filter bank, which enable us to process arbitrary-length input signals in such a way that support preservation is guaranteed. Note that standard cosine-modulated filter banks [11], which utilize a DCT-IV-type modulation, cannot be used in combination with symmetric extension methods due to their in general non-linear-phase subband filters.

The organization of the paper is as follows. In Section 2 we briefly introduce the cosine-modulated filter bank with linear-phase subband filters and show that the subband impulse responses have different centers of symmetry. Section 3 shows (for two particular input signal lengths) how symmetric extension can be obtained by using linear-phase filters with different centers of symmetry. The result is then subsequently applied to the cosine-modulated filter bank. Section 4 derives the general solution for arbitrary lengths of the input signal. In Section 5 the influence of the symmetric extension on the preservation of the DC-component in the lowpass subband is discussed, an issue being especially important in image processing applications. Section 6 presents applications of the cosine-modulated filter bank and the proposed extension method. In particular, we look at image compression and pre-echo reduction in subband audio coding. Finally, Section 7 gives a brief conclusion.

2. Linear-phase cosine-modulated filter banks

In this section the cosine-modulated filter bank according to Refs. [3,4,13] is introduced. We consider the structure in Fig. 2 and refer to this filter bank as a $2M$-subband structure. The linear-phase analysis filters $h'_k(n)$ and $h''_k(n)$ are derived from a linear-phase prototype $p(n)$ of length N by cosine and sine modulation according to

$$h'_k(n) = \rho_k p(n) \cos\left[\frac{\pi}{M} k\left(n - \frac{N-1+M}{2}\right)\right], \quad k = 0,1,\ldots,M', \tag{1}$$

$$h''_k(n) = \rho_k p(n-M) \sin\left[\frac{\pi}{M} k\left(n - M - \frac{N-1+M}{2}\right)\right], \quad k = 1,2,\ldots,M'', \tag{2}$$

where $n = 0,\ldots,N-1+M$ and

$$\rho_k = \begin{cases} \sqrt{2} & \text{if } k = 0 \text{ or } k = M, \\ 2 & \text{otherwise,} \end{cases} \qquad M' = \begin{cases} M & \text{for } N+M \text{ odd,} \\ M-1 & \text{for } N+M \text{ even,} \end{cases} \qquad M'' = 2M - 1 - M'.$$

The corresponding linear-phase synthesis filters are

$$f'_k(n) = h'_k(N-1+M-n), \quad k = 0,1,\ldots,M', \tag{3}$$

$$f''_k(n) = -h''_k(N-1+M-n), \quad k = 1,2,\ldots,M''. \tag{4}$$

Note that the impulse responses $h''_k(n)$ and $f'_k(n)$ have M leading zeros whereas for $h'_k(n)$ and $f''_k(n)$ the last M values are zero.

Due to the linear-phase even-symmetric nature of the prototype, i.e. $p(n) = p(N-1-n)$, and the symmetry of the sine and cosine modulation in (1) and (2) we have eight possible symmetries for the impulse responses of the analysis and synthesis filters, which are given in Table 1. For the sake of simplicity we refer to the different types of symmetry with the designation given in Table 2. The synthesis filter impulse responses

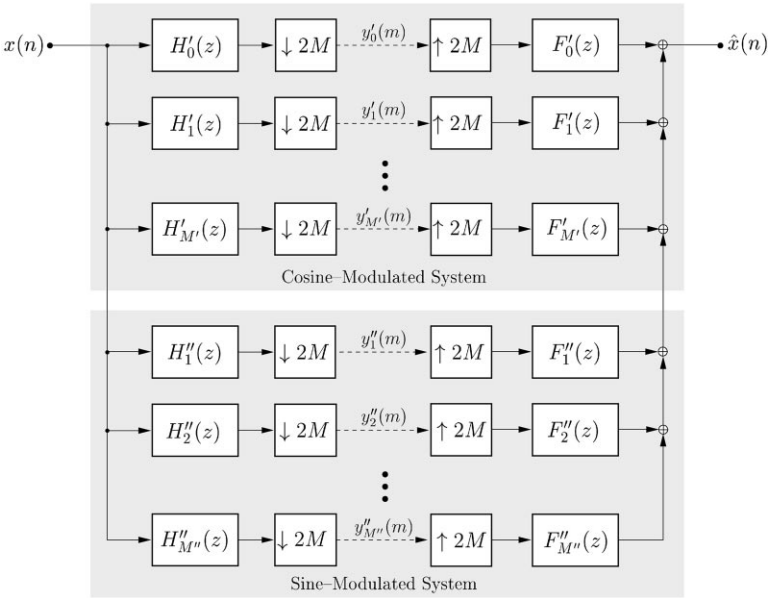

Fig. 2. Linear-phase cosine-modulated filter bank.

Table 1
Possible types of symmetry for the analysis impulse response. The prototype-length is N and $\mathbf{0}$ denotes a row vector of M zeros

		Type of symmetry	
k	Symmetry of impulse response	N even	N odd
Even	$h'_k(n) = h'_k(N-1-n)$	$[\ldots, C, B, A, A, B, C, \ldots, \mathbf{0}]$	$[\ldots, C, B, A, B, C, \ldots, \mathbf{0}]$
	$h''_k(n) = -h''_k(N-1+2M-n)$	$[\mathbf{0}, \ldots, -C, -B, -A, A, B, C, \ldots]$	$[\mathbf{0}, \ldots, -C, -B, 0, B, C, \ldots]$
Odd	$h'_k(n) = -h'_k(N-1-n)$	$[\ldots, -C, -B, -A, A, B, C, \ldots, \mathbf{0}]$	$[\ldots, -C, -B, 0, B, C, \ldots, \mathbf{0}]$
	$h''_k(n) = h''_k(N-1+2M-n)$	$[\mathbf{0}, \ldots, C, B, A, A, B, C, \ldots]$	$[\mathbf{0}, \ldots, C, B, A, B, C, \ldots]$

are the flipped versions of the corresponding analysis filters, see (3) and (4). Thus Table 1 also describes the symmetries of $f'_k(-n)$ and $f''_k(-n)$.

Due to leading or final zeros of the impulse responses, the centers of symmetry for $h'_k(n)$ and $h''_k(n)$, and also for $f'_k(n)$ and $f''_k(n)$, differ by M samples, which has to be taken into account when we wish to apply symmetric extension methods to the input signal.

3. Symmetric extension for certain input signal lengths

In this section we show (for some special cases) how symmetric extension methods can be applied to linear-phase analysis filters with different centers of symmetry. We first consider the system depicted in Fig. 3, which can be regarded as the k-th subband of the analysis filter bank with $k = 1, \ldots, M-1$. For these values

Table 2
Types of symmetry

Even symmetry	Odd symmetry	Designation in this paper
$[\ldots, C, B, A, A, B, C, \ldots]$	$[\ldots, -C, -B, -A, A, B, C, \ldots]$	AA-symmetry
$[\ldots, C, B, A, B, C, \ldots]$	$[\ldots, -C, -B, 0, B, C, \ldots]$	BAB-symmetry

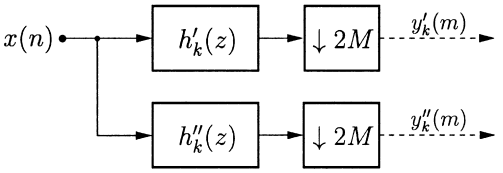

Fig. 3. Detail of the analysis filter bank with linear-phase analysis filters $h'_k(n)$ and $h''_k(n)$ having the same spectral support.

of k we have two analysis filters with the same spectral support, but different centers of symmetry as we can see from Table 1.

The necessary condition for the application of symmetric extension methods to the system in Fig. 3 is that *both* output signals $y'_k(m)$ and $y''_k(m)$ provide symmetries across the boundaries if the input signal is symmetrically extended. Clearly, the subbands for $k = 0$ and $k = M$ can be neglected in our considerations, because we have only one analysis filter and thus only one output signal. For the other values of k we will show in the following that for $y'_k(m)$ *and* $y''_k(m)$ such an output symmetry can be obtained for special input signal lengths.

3.1. *Odd-length linear-phase prototype filter, signal length* $N_x = cM + 1$

The impulse response of an odd-length linear-phase prototype has BAB-symmetry, and this also applies to the analysis impulse response. We extend our input signal at the beginning and the end by $Q = (2\ell + 1)M - (N - 1)/2$ samples, where $2\ell M > N$, $\ell \in \mathbb{N}$, using the same kind of symmetry. The extended input signal $x_{\mathrm{ex}}(n)$ is given as

$$\boldsymbol{x}_{\mathrm{ex}} = [x(Q), \ldots, x(1), x(0), x(1), \ldots, x(N_x - 2), x(N_x - 1), x(N_x - 2), \ldots, x(N_x - Q - 1)]^{\mathrm{T}}. \tag{5}$$

Both output signals $y'_k(m)$ and $y''_k(m)$ are symmetric with regard to the boundaries if the input signal has length $N_x = cM + 1$ with $c \in \mathbb{N}$. This is shown in the following two examples for even and odd values of c, respectively.

Example 1. The first example considers the case of even multiples of M, which restricts the length of the input signal to $N_x = 2cM + 1$, $c \in \mathbb{N}$. The input signal length is chosen as $N_x = 13$, the prototype filter length as $N = 5$ and the decimation factor as $2M = 4$, leading to $Q = 8$.

In Fig. 4(a), the result of the convolution in the upper branch of the system in Fig. 3 is shown, where the subsampling by factor $2M = 4$ is already introduced in the shift of the reversed filter impulse response

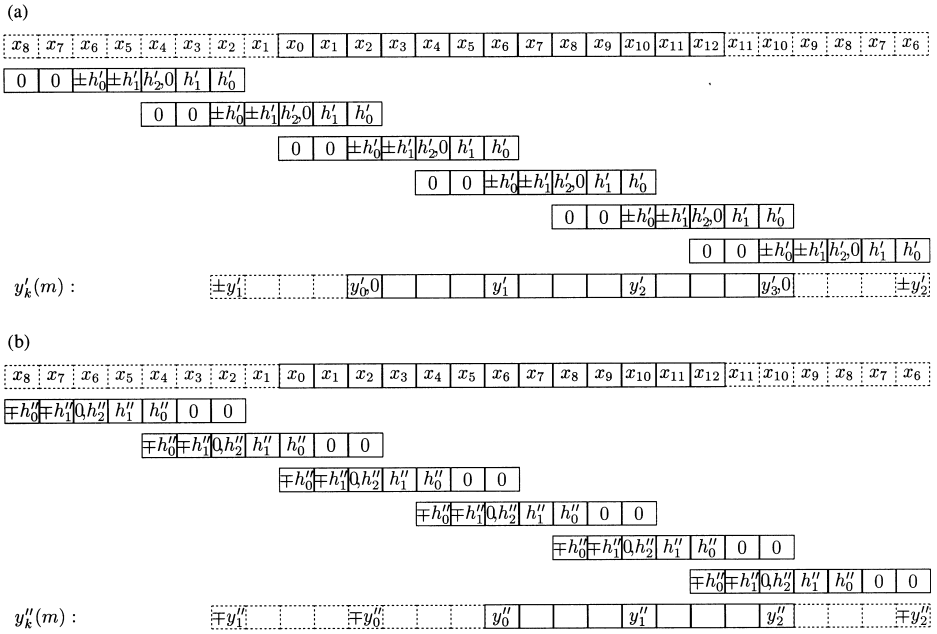

Fig. 4. Symmetries of decimated output signals $y'_k(m)$ and $y''_k(m)$ in the case of an input signal of length $N_x = 13$ and a linear-phase prototype filter of length $N = 5$. The subband index k is omitted for clarity. h'_n denotes $h'_k(n)$.

$h'_k(-n)$. The symmetric extension of the input signal and the redundant samples of the output signal are shown in dotted boxes. We can see that the output signal $y'_k(m)$ shows BAB-symmetry at both boundaries and that the part in the solid boxes contains all signal information. If the non-zero part of $h'_k(n)$ has an odd BAB-symmetry (as it is the case for odd k), the coefficient denoting the symmetry center (i.e. h'_2 in Fig. 4(a)) is necessarily zero due to the linear-phase property of $h'_k(n)$. Hence, the first and the last value in the solid boxes (i.e. y'_0 and y'_3 in Fig. 4(a)) will be equal to zero, too.

Fig. 4(b) shows the convolution operation in the lower branch of Fig. 3, where both, the subsampling factor $2M = 4$ and the leading zeros of the impulse response $h''_k(n)$ are considered. Note that the output signal shows AA-symmetry in this case, so that it is again possible to reduce $y''_k(m)$ to the non-redundant part shown in the solid boxes.

Example 2. In Fig. 5 symmetric output signals are derived for an input signal of length $N_x = 11$, i.e. $N_x = (2c+1)M + 1$, $c \in \mathbb{N}$. The other parameters are kept as in Example 1, that is $2M = 4$, $N = 5$.

The symmetries at the beginning of the output signals are the same as in Example 1 since they do not depend on the signal length. At the end we have AA-symmetry for $y'_k(m)$ and BAB-symmetry for $y''_k(m)$, respectively. Note that the symmetries are exactly the opposite of the ones in Example 1. Again, all information about the input signal is contained in the values surrounded by the solid boxes.

From Examples 1 and 2 it can be seen that for all input signal lengths $N_x = cM + 1$, $c \in \mathbb{N}$, symmetries occur at the beginning and the end of *both* output signals in Fig. 3, provided that the prototype filter has odd length.

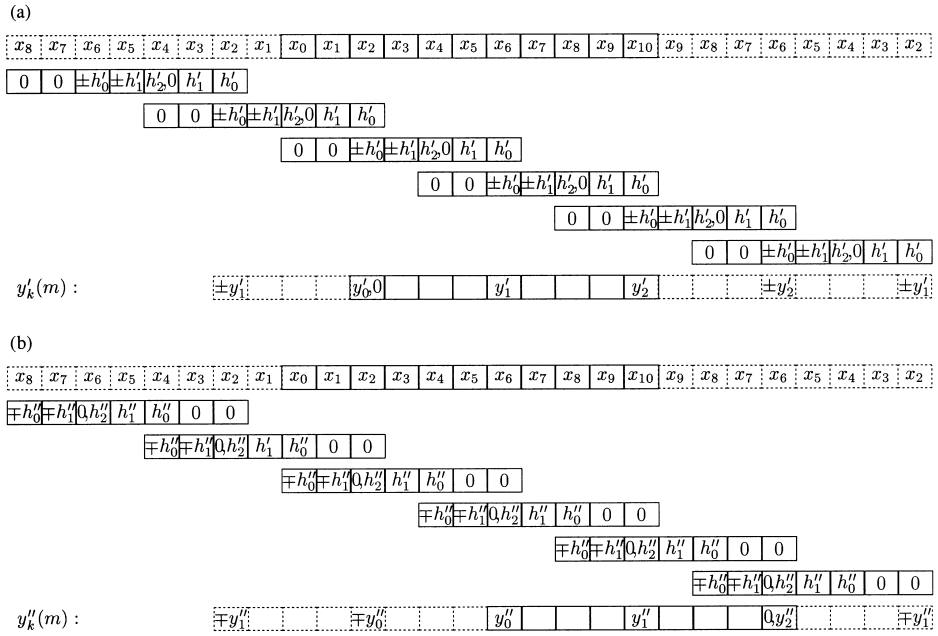

Fig. 5. Symmetries of decimated output signals $y'_k(m)$ and $y''_k(m)$ in the case of an input signal of length $N_x = 11$ and a linear-phase prototype filter of length $N = 5$. A coefficient h'_n denotes $h'_k(n)$, where the subband index k is omitted for clarity.

3.2. Even-length linear-phase prototype filter, signal length $N_x = cM$

Processing schemes for even-length linear-phase filters can be derived in a similar way as for odd-length filters. Since the impulse response of an even-length linear-phase prototype has an AA-symmetry, we here extend the input signal according to

$$\boldsymbol{x}_{\mathrm{ex}} = [x(Q-1), \ldots, x(1), x(0), x(0), \ldots, x(N_x-1), x(N_x-1), \ldots, x(N_x-Q)]^{\mathrm{T}} \tag{6}$$

with $Q = (2\ell+1)M - N/2$ and $2\ell M > N$. As in the odd-length case it can easily be shown that both output signals are symmetric for input signals of length $N_x = cM$, $c \in \mathbb{N}$.

3.3. Application to cosine-modulated filter banks

So far, we have seen that we obtain symmetries in the subband signals for special input lengths. These symmetries can be utilized to achieve support preservation with the linear-phase cosine-modulated filter bank. In the following, we have a closer look at the most important cases.

3.3.1. Special cases $N_x = 2cM + 1$ and $N_x = 2cM$

We first discuss the cases where the input signal length is fixed to $N_x = 2cM + 1$ for odd-length prototypes and to $N_x = 2cM$ for even-length prototypes, respectively. The subband matrices $\boldsymbol{Y}'$ and $\boldsymbol{Y}''$ that contain the

decimated signals $y'_k(m)$, $k = 0, \ldots, M'$ and $y''_k(m)$, $k = 1, \ldots, M''$ are given as

$$\boldsymbol{Y}' = \begin{bmatrix} \cdots & y'_0(1) & y'_0(0) & y'_0(1) & \cdots & y'_0(c-1) & y'_0(c) & y'_0(c-1) & \cdots \\ \cdots & -y'_1(1) & 0 & y'_1(1) & & y'_1(c-1) & 0 & -y'_1(c-1) & \cdots \\ \cdots & y'_2(1) & y'_2(0) & y'_2(1) & \cdots & y'_2(c-1) & y'_2(c) & y'_2(c-1) & \cdots \\ & \vdots & \vdots & \vdots & & \vdots & \vdots & \vdots & \\ \cdots & \pm y'_{M'}(1) & \begin{matrix} y'_{M'}(0) \\ 0 \end{matrix} & y'_{M'}(1) & & y'_{M'}(c-1) & \begin{matrix} y'_{M'}(c) \\ 0 \end{matrix} & \pm y'_{M'}(c-1) & \cdots \end{bmatrix}, \tag{7}$$

$$\boldsymbol{Y}'' = \begin{bmatrix} \cdots & y''_1(1) & y''_1(0) & y''_1(0) & y''_1(1) & \cdots & y''_1(c-1) & y''_1(c-1) & y''_1(c-2) & \cdots \\ \cdots & -y''_2(1) & -y''_2(0) & y''_2(0) & y''_2(1) & & y''_2(c-1) & -y''_2(c-1) & -y''_2(c-2) & \cdots \\ \cdots & y''_3(1) & y''_3(0) & y''_3(0) & y''_3(1) & \cdots & y''_3(c-1) & y''_3(c-1) & y''_3(c-2) & \cdots \\ & \vdots & & \vdots & \vdots & & \vdots & & \vdots & \\ \cdots & \pm y''_{M''}(1) & \pm y''_{M''}(0) & y''_{M''}(0) & y''_{M''}(1) & & y''_{M''}(c-1) & \pm y''_{M''}(c-1) & \pm y''_{M''}(c-2) & \cdots \end{bmatrix}, \tag{8}$$

where we assume that the input signal has been extended according to (5) and (6), respectively. Note that the boundary symmetries discussed previously can again be found in the subband matrices. Since the boundary symmetries between adjacent subbands change from even to odd and vice versa in both subband matrices, we have positive signs in the last rows of $\boldsymbol{Y}'$ for even M' and in $\boldsymbol{Y}''$ for odd M''. In $\boldsymbol{Y}'$ the values $y'_{M'}(0)$ and $y'_{M'}(c)$ are identically zero if M' is odd. The non-redundant parts of $\boldsymbol{Y}'$ and $\boldsymbol{Y}''$ are shown inside the dotted boxes. The number of non-redundant samples per subband depends on the symmetry of the impulse response. In $\boldsymbol{Y}''$ all rows (i.e. subbands) have c non-redundant samples, so that we can always cut out a rectangular block of

Table 3
Number of non-redundant samples (# nrs) in $\boldsymbol{Y}'$ and $\boldsymbol{Y}''$ for input signals of length $N_x = 2cM + 1$ and $N_x = 2cM$, $c \in \mathbb{N}$

	N even, M even	N even, M odd	N odd, M even	N odd, M odd
N_x	$2cM$	$2cM$	$2cM + 1$	$2cM + 1$
$N + M$	Even	Odd	Odd	Even
M'	$M - 1$	M	M	$M - 1$
M''	M	$M - 1$	$M - 1$	M
# nrs $\boldsymbol{Y}'$	$(c + 1)M/2 + (c - 1)M/2$	$(c + 1)(M + 1)/2 + (c - 1)(M + 1)/2$	$(c + 1)(M + 2)/2 + (c - 1)M/2$	$(c + 1)(M + 1)/2 + (c - 1)(M - 1)/2$
# nrs $\boldsymbol{Y}''$	cM	$c(M - 1)$	$c(M - 1)$	cM
# nrs total	$2cM$	$2cM$	$2cM + 1$	$2cM + 1$

Table 4
Number of non-redundant samples (# nrs) in $\boldsymbol{Y}'$ and $\boldsymbol{Y}''$ for input signals of length $N_x = (2c+1)M+1$ or $N_x = (2c+1)M$

	N even, M even	N even, M odd	N odd, M even	N odd, M odd
N_x	$(2c+1)M$	$(2c+1)M$	$(2c+1)M+1$	$(2c+1)M+1$
$N+M$	Even	Odd	Odd	Even
M'	$M-1$	M	M	$M-1$
M''	M	$M-1$	$M-1$	M
# nrs $\boldsymbol{Y}'$	$(c+1)M/2$ $+cM/2$	$(c+1)(M+1)/2$ $+c(M+1)/2$	$(c+1)(M+2)/2$ $+cM/2$	$(c+1)(M+1)/2$ $+c(M-1)/2$
# nrs $\boldsymbol{Y}''$	$(c+1)M/2$ $+cM/2$	$(c+1)(M-1)/2$ $+c(M-1)/2$	$(c+1)M/2$ $+c(M-2)/2$	$(c+1)(M+1)/2$ $+c(M-1)/2$
# nrs total	$(2c+1)M$	$(2c+1)M$	$(2c+1)M+1$	$(2c+1)M+1$

size $M''\times c$ as the non-redundant part. In $\boldsymbol{Y}'$ however, the number of non-redundant samples per subband is alternately $(c+1)$ and $(c-1)$. Table 3 shows that for both odd and even prototype lengths we end up with exactly N_x samples inside both dotted boxes. Thus, the linear-phase cosine-modulated filter bank is support-preservative for input signal lengths $N_x = 2cM$, $c\in\mathbb{N}$, when using an even-length prototype, and for $N_x = 2cM+1$ when using an odd-length prototype.

3.3.2. Special cases $N_x = (2c+1)M+1$ and $N_x = (2c+1)M$

Now we consider the cases where we either have an input signal of length $N_x = (2c+1)M+1$ and an odd-length prototype, or an input signal of length $N_x = (2c+1)M$ and an even-length prototype. Taking the symmetries of the decimated signals in Fig. 5 into account, the subband matrices $\boldsymbol{Y}'$ and $\boldsymbol{Y}''$ are now given as

$$\boldsymbol{Y}' = \begin{bmatrix} \cdots & y'_0(1) & y'_0(0) & y'_0(1) & \cdots & y'_0(c-1) & y'_0(c) & y'_0(c) & y'_0(c-1) & \cdots \\ \cdots & -y'_1(1) & 0 & y'_1(1) & & y'_1(c-1) & y'_1(c) & -y'_1(c) & -y'_1(c-1) & \cdots \\ \cdots & y'_2(1) & y'_2(0) & y'_2(1) & \cdots & y'_2(c-1) & y'_2(c) & y'_2(c) & y'_2(c-1) & \cdots \\ & \vdots & \vdots & \vdots & & \vdots & \vdots & & \vdots & \\ \cdots & \pm y'_{M'}(1) & y'_{M'}(0) & y'_{M'}(1) & & y'_{M'}(c-1) & y'_{M'}(c) & \pm y'_{M'}(c) & \pm y'_{M'}(c-1) & \cdots \\ & & 0 & & & & & & & \end{bmatrix}, \quad (9)$$

$$\boldsymbol{Y}'' = \begin{bmatrix} \cdots & y''_1(1) & y''_1(0) & y''_1(0) & y''_1(1) & \cdots & y''_1(c-1) & y''_1(c) & y''_1(c-1) & \cdots \\ \cdots & -y''_2(1) & -y''_2(0) & y''_2(0) & y''_2(1) & & y''_2(c-1) & 0 & -y''_2(c-1) & \cdots \\ \cdots & y''_3(1) & y''_3(0) & y''_3(0) & y''_3(1) & \cdots & y''_3(c-1) & y''_3(c) & y''_3(c-1) & \cdots \\ & \vdots & & \vdots & \vdots & & \vdots & \vdots & & \\ \cdots & \pm y''_{M''}(1) & \pm y''_{M''}(0) & y''_{M''}(0) & y''_{M''}(1) & & y''_{M''}(c-1) & y''_{M''}(c) & \pm y''_{M''}(c-1) & \cdots \\ & & & & & & & 0 & & \end{bmatrix}. \quad (10)$$

Again, the non-redundant subband samples are found in the dotted boxes. The upper sign in the last row of $\boldsymbol{Y}'$ is valid for even M' and the one in $\boldsymbol{Y}''$ is valid for odd M''. Note that in contrast to the cases discussed in Section 3.3.1, the number of non-redundant samples per subband amounts to c in even rows and $(c+1)$ in odd rows of $\boldsymbol{Y}'$ and $\boldsymbol{Y}''$. Table 4 gives an overview of the total number of non-redundant samples in $\boldsymbol{Y}'$ and $\boldsymbol{Y}''$, depending on the choice of N and M. It shows that the linear-phase cosine-modulated filter bank is support-preservative for input signals of length $N_x = (2c+1)M + 1$ when using an odd-length prototype and of length $N_x = (2c+1)M$ for an even-length prototype.

3.4. Matrix formulation of symmetric extension

In order to discuss the effects of the symmetric extension on the properties of the subband signals it is more convenient to describe the analysis and synthesis filtering operations with block convolution matrices.

When the linear-phase prototype is designed in such a way that the filter bank yields PR for an infinite length input signal we address the paraunitary case. The application of the filter bank to a length N_x input signal $\boldsymbol{x}$ can then be viewed as an orthonormal transform $\boldsymbol{y} = \boldsymbol{H}\boldsymbol{x}$, with a size $N_x \times N_x$ transform matrix $\boldsymbol{H}$ satisfying $\boldsymbol{H}^{\mathrm{T}}\boldsymbol{H} = \boldsymbol{I}$.

In the following discussion we restrict ourselves to the case of even-length prototype filters and input signal lengths of $N_x = 2cM$, $c \in \mathbb{N}$. However, the extensions to $N_x = (2c+1)M$ and to odd-length prototypes are straightforward.

A vector $\boldsymbol{y}$ lining up all columns inside the dotted boxes of (7) and (8), i.e. containing all non-redundant subband samples, can be obtained by multiplication of the extended input signal

$$\boldsymbol{x}_{\mathrm{ex}} = [x(N/2+M-1), \ldots, x(1), x(0), x(0), \ldots, x(N_x-1), x(N_x-1), \ldots, x(N_x-N/2)]^{\mathrm{T}} \tag{11}$$

with a convolution matrix $\boldsymbol{H}$ of size $N_x \times (N_x + N + M)$, which has the following structure:

$$\boldsymbol{H} = \begin{bmatrix} \hat{\mathscr{H}}' & & & & \boldsymbol{0} \\ 2M\ \mathscr{H} & & & & \\ & \mathscr{H} & & & \\ & & \ddots & & \\ & & & \mathscr{H} & \\ & & & & \hat{\mathscr{H}}' \\ \boldsymbol{0} & & & & \mathscr{H}'' \end{bmatrix}.$$

The sub-matrices $\mathscr{H}$ and $\mathscr{H}''$ contain the flipped analysis impulse responses:

$$\mathscr{H} = \begin{bmatrix} \mathscr{H}' \\ \mathscr{H}'' \end{bmatrix} \quad \text{with } \mathscr{H}' = \begin{bmatrix} h'_0(N-1+M) & h'_0(N-2+M) & \cdots & h'_0(0) \\ h'_1(N-1+M) & h'_1(N-2+M) & \cdots & h'_1(0) \\ \vdots & \vdots & \ddots & \vdots \\ h'_{M'}(N-1+M) & h'_{M'}(N-2+M) & \cdots & h'_{M'}(0) \end{bmatrix},$$

$$\mathscr{H}'' = \begin{bmatrix} h''_1(N-1+M) & h''_1(N-2+M) & \cdots & h''_1(0) \\ h''_2(N-1+M) & h''_2(N-2+M) & \cdots & h''_2(0) \\ \vdots & \vdots & \ddots & \vdots \\ h''_{M''}(N-1+M) & h''_{M''}(N-2+M) & \cdots & h''_{M''}(0) \end{bmatrix}.$$

Since every second subband sample in the first and last column in the dotted box of $\boldsymbol{Y}'$ in (7) is zero, we have to consider only every second analysis impulse response $h'_k(n)$ at the left and right boundary of the input signal. Thus, the sub-matrix $\hat{\mathscr{H}}'$ of dimension $(\lfloor M'/2 \rfloor + 1) \times (M+N)$ is given as

$$\hat{\mathscr{H}}' = \begin{bmatrix} h'_0(N-1+M) & h'_0(N-2+M) & \cdots & h'_0(0) \\ h'_2(N-1+M) & h'_2(N-2+M) & \cdots & h'_2(0) \\ \vdots & \vdots & \ddots & \vdots \\ h'_{2\cdot\lfloor M'/2 \rfloor}(N-1+M) & h'_{2\cdot\lfloor M'/2 \rfloor}(N-2+M) & \cdots & h'_{2\cdot\lfloor M'/2 \rfloor}(0) \end{bmatrix}. \tag{12}$$

All non-redundant subband samples are now acquired by $\boldsymbol{y} = \boldsymbol{H}\boldsymbol{x}_{\mathrm{ex}}$.

Since the filter bank is paraunitary when applied to infinite-length signals, the analysis impulse responses are pairwise orthogonal and also orthogonal to their shifted versions (shifts by multiples of $2M$). These impulse responses form the rows of the rectangular matrix $\boldsymbol{H}$ such that

$$\boldsymbol{h}_i^{\mathrm{T}} \boldsymbol{h}_k = \delta_{ik}, \quad i,k = 0,\ldots,N_x - 1, \tag{13}$$

where δ_{ik} denotes the Kronecker symbol and $\boldsymbol{h}_i^{\mathrm{T}}$ denotes the i-th row of $\boldsymbol{H}$.

Instead of symmetrically extending the input signal $\boldsymbol{x}$ as in (11), we can also apply the symmetric extension operation to the analysis filters at the boundaries of the matrix $\boldsymbol{H}$. This can be carried out by postmultiplying the block convolution matrix $\boldsymbol{H}$ with a $(N_x + N + M) \times N_x$ matrix

$$\boldsymbol{E}_h = \begin{bmatrix} \boldsymbol{K}_1 \\ \boldsymbol{I}_{N_x} \\ \boldsymbol{K}_2 \end{bmatrix},$$

where $\boldsymbol{K}_1$ and $\boldsymbol{K}_2$ denote reflection matrices

$$[\boldsymbol{K}_1]_{i,\ell} = \delta_{M+N/2-1-i,\ell}, \quad i = 0,\ldots,N/2+M-1, \quad \ell = 0,\ldots,N_x-1,$$

$$[\boldsymbol{K}_2]_{i,\ell} = \delta_{N_x-1-i,\ell}, \quad i = 0,\ldots,N/2-1, \quad \ell = 0,\ldots,N_x-1.$$

This leads to a new $N_x \times N_x$ analysis transform matrix $\boldsymbol{H}_{N_x} = \boldsymbol{H}\boldsymbol{E}_h$ and an analysis of the form $\boldsymbol{y} = \boldsymbol{H}_{N_x}\boldsymbol{x}$.

Using (13) and the symmetries of the linear-phase even-length analysis filters, one can prove that the rows of $\boldsymbol{H}_{N_x}$ are still orthogonal, but not orthonormal, i.e.

$$\boldsymbol{h}_{N_x,i}^{\mathrm{T}} \boldsymbol{h}_{N_x,k} = c_i \delta_{ik}, \quad i,k = 0,\ldots,N_x-1 \tag{14}$$

with

$$c_i = \begin{cases} 2 & \text{for } i = 0,\ldots,\lfloor M'/2 \rfloor \text{ and } i = N_x - 1 - M'' - \lfloor M'/2 \rfloor,\ldots,N_x - 1 - M'', \\ 1 & \text{otherwise.} \end{cases} \tag{15}$$

Thus, the input signal can be reconstructed according to

$$\hat{\boldsymbol{x}} = \boldsymbol{F}_{N_x}^{\mathrm{T}} \boldsymbol{y} \quad \text{with } \boldsymbol{F}_{N_x} = \mathrm{diag}\{[c_0, c_1, \ldots, c_{N_x-1}]\}^{-1} \boldsymbol{H}_{N_x}. \tag{16}$$

From (14) and (15) we see that the energies of some filters are increased by a factor two.

Construction of an orthonormal transform: An orthonormal transform with all $c_i = 1$, $i = 0, \ldots, N_x - 1$, can be obtained by proper scaling of the analysis and synthesis transform matrices. This can be carried out by multiplying $\boldsymbol{H}_{N_x}$ with a size $N_x \times N_x$ diagonal matrix $\boldsymbol{D} = \mathrm{diag}\{[1/\sqrt{c_0}, 1/\sqrt{c_1}, \ldots, 1/\sqrt{c_{N_x-1}}]\}$ according to

$$\boldsymbol{H}_{\mathrm{o}} = \boldsymbol{D}\boldsymbol{H}_{N_x} = \boldsymbol{D}^{-1}\boldsymbol{F}_{N_x}, \tag{17}$$

so that $\boldsymbol{H}_{\mathrm{o}}\boldsymbol{H}_{\mathrm{o}}^{\mathrm{T}} = \boldsymbol{H}_{\mathrm{o}}^{\mathrm{T}}\boldsymbol{H}_{\mathrm{o}} = \boldsymbol{I}_{N_x}$ is satisfied.

4. Symmetric extension for arbitrary input-signal lengths

4.1. Problem statement

In the last section we have shown that the linear-phase cosine-modulated filter bank can be support-preservative for input signals of length $N_x = cM + 1$ and $N_x = cM$, $c \in \mathbb{N}$, depending on the prototype length. In order to recover the symmetries within the subbands for arbitrary-length input signals, we propose the following procedure:

In a first step, we extend the input signal vector $\boldsymbol{x}$ with N_a values $a(n)$ to the length $N_{\tilde{x}} = \tilde{c}M$ or $N_{\tilde{x}} = \tilde{c}M + 1$. We thus obtain the new input signal $\tilde{x}(n)$, which can be written as a vector $\tilde{\boldsymbol{x}}$ according to

$$\tilde{\boldsymbol{x}} = [a(0), \ldots, a(N_{a_1} - 1), x(0), \ldots, x(N_x - 1), a(N_{a_1}), \ldots, a(N_a - 1)]^{\mathrm{T}} \tag{18}$$

with $N_a = N_{\tilde{x}} - N_x$, $0 \leqslant N_{a_1} \leqslant N_a$. A possible choice for $N_{\tilde{x}}$ is given by

$$N_{\tilde{x}} = \begin{cases} \tilde{c}M + 1, & \tilde{c} = \lfloor \frac{N_x - 2}{M} \rfloor + 1 \text{ for odd prototype length,} \\ \tilde{c}M, & \tilde{c} = \lfloor \frac{N_x - 1}{M} \rfloor + 1 \text{ for even prototype length.} \end{cases} \tag{19}$$

The effect of this first step is that for even $\tilde{c}$ we obtain the subband matrices $\boldsymbol{Y}'$ and $\boldsymbol{Y}''$ depicted in (7) and (8), respectively, and for odd $\tilde{c}$ those shown in (9) and (10). Thus, by extension of the original signal vector according to (18) we can again exploit the symmetries discussed for the special cases in Section 3.3.1 and Section 3.3.2. However, there is still one drawback with this solution: The resulting filter bank is not support-preservative, since the number of non-redundant subband samples is now $N_{\tilde{x}}$, which is N_a samples more than the length N_x of our original input signal.

Support preservation can again be achieved, when the number of non-redundant samples in both $\boldsymbol{Y}'$ and $\boldsymbol{Y}''$ is reduced by N_a samples. For this the extra values $a(n)$ may be chosen in such a way that they lead to N_a pre-defined values in the subband matrices, denoted as $k(n)$, $n = 0, \ldots, N_a - 1$. The pre-defined values are known in the receiver and do not need to be transmitted.

The additional N_a pre-defined samples may appear at all positions within $\boldsymbol{Y}'$ and $\boldsymbol{Y}''$ that are influenced by the introduced values $a(n)$ during convolution and subsampling. Possible choices for their placement are

- in the first or last column inside the dotted boxes of $\boldsymbol{Y}'$ and $\boldsymbol{Y}''$,
- if $\tilde{c}$ is even, in the first columns of $\boldsymbol{Y}'$ in (7) just outside the dotted box (and thus also the corresponding values inside the dotted box),
- if $\tilde{c}$ is odd, in the first column of $\boldsymbol{Y}'$ in (9) on the left-hand side and the first column of $\boldsymbol{Y}''$ in (10) on the righthand side of the dotted box.

N_{a_1} samples may be placed in the first columns and $N_a - N_{a_1}$ samples in the last columns of the dotted boxes in $\boldsymbol{Y}'$ and $\boldsymbol{Y}''$, respectively. However, the actual choice may depend on different aspects:

- The variance of the subband signals at the boundaries should not be changed too much by the inserted values and the symmetric extension.

- It might be disadvantageous for subband coding to have too many different subband signal lengths, e.g. when a zig-zag scanning over the subbands is required (as for example in the JPEG image coding scheme [7]).
- In real-time applications with fixed-point arithmetic it might cause problems if the inserted values $a(n)$ are not in the same range as the input signal $x(n)$.

4.2. Solution

In the following we show that the inserted values $a(n)$ can be determined by solving a system of linear equations. The matrix formulation for the convolution can be given similarly to the solution in the last section when replacing N_x by $N_{\tilde{x}}$ for the matrix and vector dimensions, as

$$\tilde{\boldsymbol{y}} = \boldsymbol{H}_{N_{\tilde{x}}}\tilde{\boldsymbol{x}}. \tag{20}$$

Here $\tilde{\boldsymbol{y}}$ is of length $N_{\tilde{x}}$ and still contains the predetermined values $k(n)$, $n = 0, \ldots, N_a - 1$, from which N_{a_1} values can be arbitrarily positioned within the first and $N_a - N_{a_1}$ values within the last values of $\tilde{\boldsymbol{y}}$. For reasons of simplicity, we here choose $N_{a_1} = 0$ and $\tilde{\boldsymbol{y}} = [\boldsymbol{y}^{\mathrm{T}}, \boldsymbol{k}^{\mathrm{T}}]^{\mathrm{T}}$, where $\boldsymbol{y}$ contains the N_x non-redundant subband samples and $\boldsymbol{k} = [k(0), k(1), \ldots, k(N_a - 1)]^{\mathrm{T}}$. The system of linear equations is then given by

$$\begin{bmatrix} \boldsymbol{y} \\ \boldsymbol{k} \end{bmatrix} = \begin{bmatrix} \boldsymbol{H}_{00} & \boldsymbol{H}_{01} \\ \boldsymbol{H}_{10} & \boldsymbol{H}_{11} \end{bmatrix} \begin{bmatrix} \boldsymbol{x} \\ \boldsymbol{a} \end{bmatrix} \tag{21}$$

with

$$[\boldsymbol{H}_{00}]_{i,\ell} = [\boldsymbol{H}_{N_{\tilde{x}}}]_{i,\ell}, \quad i, \ell = 0, \ldots, N_x - 1,$$

$$[\boldsymbol{H}_{01}]_{i,\ell} = [\boldsymbol{H}_{N_{\tilde{x}}}]_{i,N_x+\ell}, \quad i = 0, \ldots, N_x - 1,\ \ell = 0, \ldots, N_a - 1,$$

$$[\boldsymbol{H}_{10}]_{i,\ell} = [\boldsymbol{H}_{N_{\tilde{x}}}]_{N_x+i,\ell}, \quad i = 0, \ldots, N_a - 1,\ \ell = 0, \ldots, N_x - 1,$$

$$[\boldsymbol{H}_{11}]_{i,\ell} = [\boldsymbol{H}_{N_{\tilde{x}}}]_{N_x+i,N_x+\ell}, \quad i, \ell = 0, \ldots, N_a - 1.$$

Note that this special case can be derived from the general case with $N_{a_1} \neq 0$ and a different placement of $k(n)$ inside $\tilde{\boldsymbol{y}}$ by introduction of a permutation matrix that rearranges the rows of $\tilde{\boldsymbol{y}}$ and $\boldsymbol{H}_{N_{\tilde{x}}}$.

Given the vector $\boldsymbol{k}$, the solution for $\boldsymbol{a}$ writes

$$\boldsymbol{a} = \boldsymbol{H}_{11}^{-1}(\boldsymbol{k} - \boldsymbol{H}_{10}\boldsymbol{x}), \tag{22}$$

and the relationship between the non-redundant subband samples $\boldsymbol{y}$, the input vector $\boldsymbol{x}$ and the pre-defined subband values $\boldsymbol{k}$ is given by

$$\boldsymbol{y} = \underbrace{(\boldsymbol{H}_{00} - \boldsymbol{H}_{01}\boldsymbol{H}_{11}^{-1}\boldsymbol{H}_{10})}_{\boldsymbol{H}_b}\boldsymbol{x} + \boldsymbol{H}_{01}\boldsymbol{H}_{11}^{-1}\boldsymbol{k}. \tag{23}$$

Likewise, the reconstructed signal $\hat{\boldsymbol{x}}$ can be obtained from

$$\begin{bmatrix} \hat{\boldsymbol{x}} \\ \hat{\boldsymbol{a}} \end{bmatrix} = \begin{bmatrix} \boldsymbol{F}_{00} & \boldsymbol{F}_{01} \\ \boldsymbol{F}_{10} & \boldsymbol{F}_{11} \end{bmatrix}^{\mathrm{T}} \begin{bmatrix} \boldsymbol{y} \\ \boldsymbol{k} \end{bmatrix} \tag{24}$$

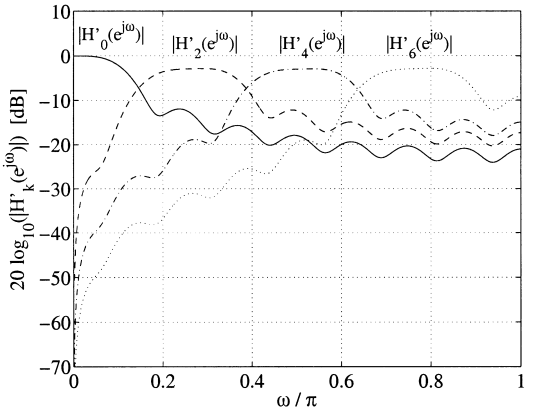

Fig. 6. Frequency responses for the first four boundary filters in $\boldsymbol{H}_b$. $N_{a_1} = 0$, $M = 8$, and an ELT prototype are used.

with

$$[\boldsymbol{F}_{00}]_{i,\ell} = [\boldsymbol{F}_{N_{\tilde{x}}}]_{i,\ell}, \qquad i,\ell = 0,\ldots,N_x - 1,$$
$$[\boldsymbol{F}_{01}]_{i,\ell} = [\boldsymbol{F}_{N_{\tilde{x}}}]_{i,N_x+\ell}, \qquad i = 0,\ldots,N_x - 1,\ \ell = 0,\ldots,N_a - 1,$$
$$[\boldsymbol{F}_{10}]_{i,\ell} = [\boldsymbol{F}_{N_{\tilde{x}}}]_{N_x+i,\ell}, \qquad i = 0,\ldots,N_a - 1,\ \ell = 0,\ldots,N_x - 1,$$
$$[\boldsymbol{F}_{11}]_{i,\ell} = [\boldsymbol{F}_{N_{\tilde{x}}}]_{N_x+i,N_x+\ell}, \quad i,\ell = 0,\ldots,N_a - 1$$

as

$$\hat{\boldsymbol{x}} = \boldsymbol{F}_{00}^{\mathrm{T}}\boldsymbol{y} + \boldsymbol{F}_{10}^{\mathrm{T}}\boldsymbol{k}. \tag{25}$$

Note that this method can as well be applied to a periodic extension of arbitrary-length input signals. This only requires a matrix formulation similar to Section 3.4, where the resulting convolution matrices then replace $H_{N_{\tilde{x}}}$ in (21) and $F_{N_{\tilde{x}}}$ in (24), respectively.

The special case $\boldsymbol{k} = \boldsymbol{0}$: For $\boldsymbol{k} = \boldsymbol{0}$ it is possible to write (23) and (25) in terms of size $N_x \times N_x$ analysis and synthesis transform matrices $\boldsymbol{H}_b$ and $\boldsymbol{F}_b$, respectively:

$$\boldsymbol{H}_b = \boldsymbol{H}_{00} - \boldsymbol{H}_{01}\boldsymbol{H}_{11}^{-1}\boldsymbol{H}_{10} \in \mathbb{R}^{N_x \times N_x}, \quad \boldsymbol{F}_b = \boldsymbol{F}_{00}^{\mathrm{T}}, \tag{26}$$

where $\boldsymbol{F}_b^{\mathrm{T}}\boldsymbol{H}_b = \boldsymbol{I}_{N_x}$.

Note that the transform matrices $\boldsymbol{F}_b$ and $\boldsymbol{H}_b$ are generally not orthogonal to themselves, but the biorthogonality relation $\boldsymbol{f}_{b_i}^{\mathrm{T}}\boldsymbol{h}_{b_k} = \delta_{ik}$, $i,k = 0,\ldots,N_x - 1$ holds between the column vectors $\boldsymbol{f}_{b_i}$ and $\boldsymbol{h}_{b_i}$ of $\boldsymbol{F}_b$ and $\boldsymbol{H}_b$, respectively. Thus, the underlying filter bank generally becomes biorthogonal when using a linear-phase PR prototype and processing finite signals of lengths $N_x \neq cM$, $c \in \mathbb{N}$. This is evident, since inserting $N_a = N_{\tilde{x}} - N_x$ additional non-zero samples into the input signal increases the energy of the subband signals compared to an input signal of length N_x.

Boundary frequency responses: To illustrate the frequency selectivity of the boundary filters, we consider a filter bank with $M = 8$ and an extended lapped transform (ELT) prototype from Malvar [15] of length $N = 4M$. The parameter N_{a_1} is chosen as $N_{a_1} = 0$. The magnitude frequency responses of the first four boundary filters on the left boundary in $\boldsymbol{H}_b$ (these are the filters in $\widehat{\mathscr{H}}'$, see (12)) are depicted in Fig. 6. We can see that these filters are fairly frequency selective. However, it should be noted that their performance degrades for $N_{a_1} > 0$.

5. Influence on the DC-component

In subband coding of images it is important that the DC component of the input signal is kept in the lowpass subband. We thus require all analysis filters (except the lowpass filter) to have one or more zeros at $z = 1$, or at least a sufficiently high stopband attenuation for $\omega = 0$, which prevents the DC from leaking to other subbands. Otherwise quantization of the subband samples would cause a DC input not to be reconstructed as pure DC, which may lead to a noticeable degradation of the reconstructed signal. When processing finite length signals (e.g. images) these requirements also must hold for the boundary filters of the filter bank.

For a constant input signal $\boldsymbol{x}_c$ of length $N_x = 2cM$ the analysis based on the extension method results in a constant DC value in the lowest subband, while all other subbands are zero due to the zeros of the analysis filters at $z = 1$. On the other hand, when using the orthonormalized filter bank described in Eq. (17), the DC amplification in the lowest band changes at the boundaries by factor $\frac{1}{\sqrt{2}}$. Thus, if we want to maintain the ideal DC behavior in the lowest band, while achieving orthonormality for the other bands, we may replace the scaling matrix $\boldsymbol{D}$ in (17) by

$$\boldsymbol{D}_d = \mathrm{diag}\left\{\left[1, \frac{1}{\sqrt{c_1}}, \ldots, \frac{1}{\sqrt{c_q}}, 1, \frac{1}{\sqrt{c_{q+2}}}, \ldots, \frac{1}{\sqrt{c_{N_x-1}}}\right]\right\} \quad \text{with } q = N_x - 2 - M'' - \lfloor M'/2 \rfloor,$$

resulting in a transform matrix $\boldsymbol{H}_d = \boldsymbol{D}_d \boldsymbol{H}_{N_x}$. The c_i are defined as in (15) and the synthesis has to be carried out with $\boldsymbol{F}_d = \boldsymbol{D}_d^{-1} \boldsymbol{F}_{N_x}$.

For general signal lengths $(2c-1)M < N_x < 2cM$ the perfect DC behavior can be maintained by using appropriate extension values. However, for arbitrary input signals, this is not a trivial matter. To find the necessary extension values $a(n)$ one first needs to compute the DC component at the boundaries of the signal. Then, this knowledge can be applied to define the extra subband samples $k(n)$, from which finally the samples $a(n)$ can be computed.

6. Applications

6.1. Image coding example

Important applications where finite-length signals are involved are image and intraframe video compression. Utilizing a modulated filter bank for spectral decomposition in those applications has generally the advantage of reduced computational complexity compared to the widely used tree-structured systems.

As we have seen, signals of any length can be processed, so that there is no restriction on the image size. However, the image size and the distribution of extra values $a(n)$ to the left and right boundary influence the compression properties. In order to show these effects, we look at the compression of parts of the Lena image with different sizes. A filter bank with $2M = 16$ subbands and an ELT prototype of length $N = 4M$ from Malvar [15] are used. The bit allocation is carried out in a rate-distortion optimal sense according to the method presented in [19]. The entropy of the quantized subband signals amounts to 0.1 bits per pixel (bpp) in all cases.

We first consider a part of the Lena image of size 446×510. The image is shown in Fig. 7(a). Note that both 446 and 510 are not multiples of $2M$, and the rows and columns of the input image have to be extended (by two samples) prior to decomposition. As an example we choose $\boldsymbol{k} = \boldsymbol{0}$ in the following. Fig. 7(b) shows the coding result for the case where insertion takes place at the end of each row and column ($N_{a_1} = 0$) with the modified subband values $y'_6(c) = y''_{M''}(c-1) = 0$. We see that heavy artifacts at the lower and the right boundary of the reconstructed image occur. These artifacts are due to extremely large subband samples at

Fig. 7. (a) Part of original Lena image (size 446×510); (b)–(d) reconstructed Lena images with $2M = 16$, bit rate 0.1 bpp, and ELT prototype; (b) image size 446×510, insertion at the end of rows and columns with the modified subband values $y'_6(c) = y''_{M'}(c-1) = 0$, PSNR = 25 dB; (c) image size 446×510 samples, modified subband values $y'_6(c) = y''_3(c-1) = 0$, PSNR = 29 dB; (d) image size 448×512, PSNR = 29.2 dB.

these boundaries. If we choose different subband values to be modified ($y'_6(c)$ and $y''_3(c-1)$), the subband samples at the boundaries behave much better, and we achieve a much better visual quality and a higher PSNR (4 dB more). The result is shown in Fig. 7(c). Finally, the reconstruction result for an image of size 448×512 is shown in Fig. 7(d), where the introduction of additional values in the rows and columns is not necessary. The visual quality and the PSNR are comparable to the result in Fig. 7(c).

6.2. Improved representation of transient signal segments in subband audio coding

In this section, we show that the proposed extension method can be successfully applied to pre-echo reduction in subband audio coding. The problem being addressed here is that in audio subband coding, the

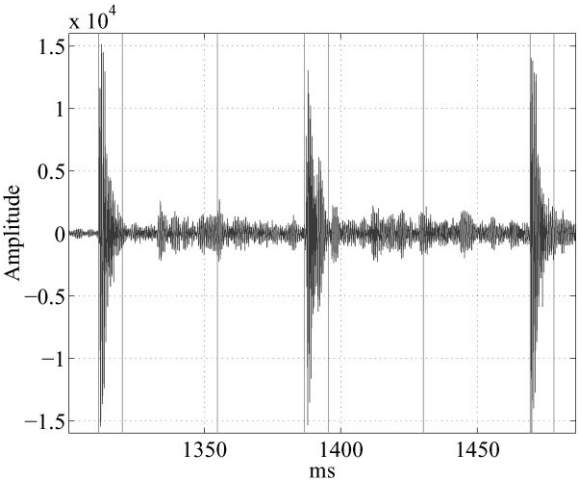

Fig. 8. Castanet signal: Adaptive framing.

frame boundaries for partitioning the input signal are usually chosen independently of the content of the audio signal. For attack-like transients (e.g. castanets, triangles, etc.) this results in audible pre-echoes, since the duration of premasking in the human auditory system can almost be neglected [26]. As a solution we use an adaptive framing strategy, where the frame boundaries are chosen so that the attacks always appear at the beginning of a segment while the segments end either in front of the next attack or in a stationary region. This framing is carried out prior to the analysis filter bank and is obtained via an energy-based criterion presented in [10].

The proposed processing scheme for linear-phase cosine-modulated filter banks allows the support-preservative decomposition of arbitrary-length signals, so that the segmentation can take place extremely close to attacks, and pre-echoes can almost completely be avoided. This is not the case for other methods based on adaptively changing the resolution of the time-frequency plane via switched filter banks as the ones in [17,21], where the frame borders are only allowed on a fixed time grid. The same holds for post-filtering of pre-echo corrupted frames as proposed in [14].

The segmentation result for an excerpt of a castanet signal is depicted in Fig. 8. The figure reveals that symmetric extension remains as the only feasible signal extension method, since especially for transient frames we most likely have completely different signal behaviors at the left and the right frame boundary.

The resulting audio coding scheme, which utilizes this adaptive framing strategy is derived from the MPEG layer 1 codec [6]. After the segmentation of the input signal the resulting (finite-length) signals are processed with the support-preservative linear-phase cosine-modulated analysis filter bank. Since the DC component in audio signals can be neglected, the extra scaling operations described in Section 5 are not necessary here, and we can simply assume the filter bank to be orthonormal. Furthermore, we restrict ourselves to an input signal length of $N_x = 2cM$, $c \in \mathbb{N}$. As mentioned earlier, this choice ensures to have well-behaved subband samples at the boundaries, and it also reduces the overall number of different frame-lengths to be transmitted to the receiver. The bit-allocations for the scalar quantization of the subband signals are calculated via a psychoacoustical model on a frame-by-frame basis.

The pre-echo suppression capabilities of this experimental audio codec are visualized in Fig. 9. In this example the number of subbands is chosen as $2M = 64$, the block-length is allowed to vary between 384 and 1536 samples, and the linear-phase prototype of length $N = 512$ is designed with the method in [9]. Fig. 9(a)

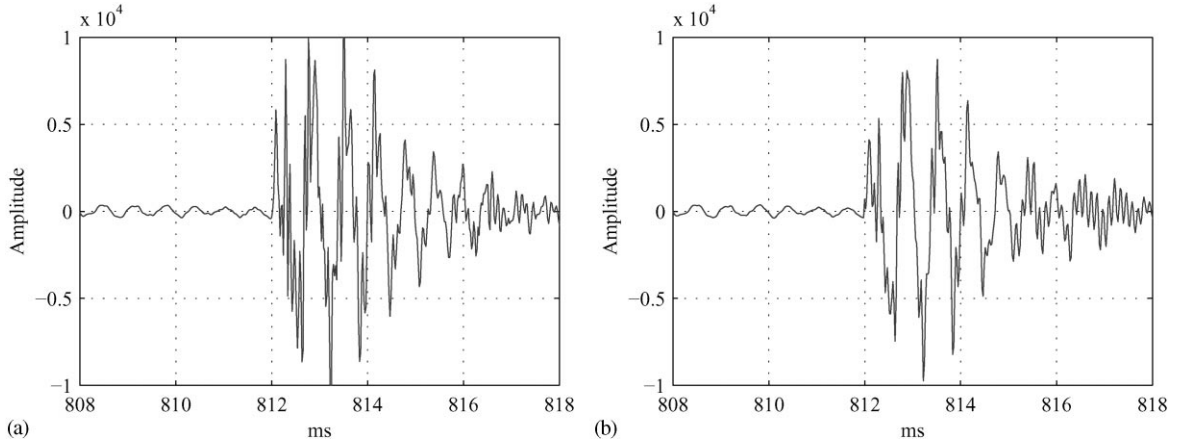

Fig. 9. (a) Original signal segment and, (b) reconstructed signal segment, coded at 75 kBit/s.

shows a transient part of the castanet signal. The reconstructed signal is displayed in Fig. 9(b), after being coded at 75 kBit/s. Nearly no pre-echo artifacts are visible in the plot of the reconstructed signal.

7. Conclusion

We have shown that it is possible to find symmetric extensions for the $2M$-band linear-phase cosine-modulated filter bank, which allow us to process finite-length signals without border distortions. Standard symmetric extension methods cannot be applied to this filter bank, because the centers of symmetry for the sine- and cosine-modulated linear-phase filters are M samples apart.

We first derived the extension method for two special cases with input signal lengths of $N_x = cM, c \in \mathbb{N}$, for even-length linear-phase prototypes and $N_x = cM + 1$ for odd-length prototypes, respectively. Based on these special cases, general solutions for arbitrary-length input signals could be obtained. The method is based on the insertion of additional values prior decomposition. The necessary modifications of the input signal influence the properties of the subband signals, where it is generally advantageous to keep the number of additional values low. Applications have been presented in audio and image coding. In audio coding it could be shown that our method allows the efficient suppression of pre-echoes via separate processing of finite-length signal blocks.

References

[1] L. Chen, T.Q. Nguyen, K.P. Chan, Symmetric extension methods for M-channel linear-phase perfect reconstruction filter banks, IEEE Trans. Signal Process. SP-43 (November 1995) 2505–2511.

[2] R.E. Crochiere, L.R. Rabiner, Multirate Digital Signal Processing, Prentice-Hall, New Jersey, 1983.

[3] R. Gopinath, Modulated filter banks and wavelets: A general unified theory, in: Proceedings of the IEEE International Conference on Acoustic, Speech, Signal Processing, Atlanta, USA, April 1996, pp. 1586–1589.

[4] P.N. Heller, T. Karp, T.Q. Nguyen, A general formulation for modulated filter banks, IEEE Trans. Signal Process. SP-47 (April 1999) 986–1002.

[5] C. Herley, M. Vetterli, Orthogonal time-varying filter banks and wavelet packets, IEEE Trans. Signal Process. SP-42 (October 1994) 2650–2663.

[6] International Organization for Standardization, Coding of Moving Pictures and Associated Audio for Digital Storage Media at up to about 1.5 MBit/s, Audio Part (11172-3), November 1992.
[7] JPEG technical specification: Revision (DRAFT), Joint Photographic Experts Group, ISO/IEC JTC1/SC2/WG8, CCITT SGVIII, August 1990.
[8] T. Karp, J. Kliewer, A. Mertins, N.J. Fliege, Processing arbitrary-length signals with MDFT filter banks, in: Proceedings of the IEEE International Conference on Acoustic, Speech, Signal Processing, Atlanta, USA, May 1996, pp. 1479–1482.
[9] J. Kliewer, Simplified design of linear-phase prototype filters for modulated filter banks, in: Proceedings of the European Signal Processing Conference, Signal Processing VIII: Theory and Applications, Trieste, Italy, September 1996, pp. 1191–1194.
[10] J. Kliewer, A. Mertins, Audio subband coding with improved representation of transient signal segments, in: Proceedings of the European Signal Processing Conference, Signal Processing IX: Theory and Applications, Rhodes, Greece, September 1998, pp. 2345–2348.
[11] R.D. Koilpillai, P.P. Vaidyanathan, Cosine-modulated FIR filter banks satisfying perfect reconstruction, IEEE Trans. Signal Process. SP-40 (April 1992) 770–783.
[12] A.N. Lemma, E.F. Deprettere, Time-varying biorthogonal filter banks: A state-space approach, IEEE Trans. on Circuits and Systems 45 (3) (March 1998) 280–289.
[13] Y. Lin, P.P. Vaidyanathan, Linear phase cosine modulated maximally decimated filter banks with perfect reconstruction, IEEE Trans. Signal Process. SP-43 (November 1995) 2525–2539.
[14] Y. Mahieux, J.P. Petit, High-quality audio transform coding at 64 kbps, IEEE Trans. Commun. 42 (11) (November 1994) 3010–3019.
[15] H.S. Malvar, Signal Processing with Lapped Transforms, Artech House, Norwood, 1992.
[16] A. Mertins, Time-varying and support preservative filter banks: design of optimal transition and boundary filters via SVD, in: Proceedings of the IEE International Conference on Acoustic Speech, Signal Processing, Detroit, USA, May 1995, pp. 1316–1319.
[17] J. Princen, J.D. Johnston, Audio coding with signal adaptive filterbanks, in: Proceedings of the IEEE International Conference on Acoustic, Speech, Signal Processing, Detroit, USA, 1995, pp. 3071–3074.
[18] R.L. de Queiroz, T.Q. Nguyen, K.R. Rao, The GenLOT: generalized linear-phase lapped transform, IEEE Trans. Signal Process. SP-44 (March 1996) 497–507.
[19] K. Ramchandran, M. Vetterli, Best wavelet packet bases in a rate–distortion sense, IEEE Trans. Image Process. 2 (2) (April 1993) 160–175.
[20] G. Schuller, Time varying filter banks with variable system delay, in: Proceedings of the IEEE International Conference on Acoustic Speech, Signal Processing, Munich, Germany, May 1997, pp. 2469–2472.
[21] D. Sinha, J.D. Johnston, Audio compression at low bit rates using a signal adaptive switched filter-bank, in: Proceedings of the IEEE International Conference on Acoustic, Speech, Signal Processing, Vol. 2, Atlanta, USA, pp. 1053–1056, 1996.
[22] M.J.T. Smith, S.L. Eddins, Analysis/synthesis techniques for subband image coding, IEEE Trans. Acoust. Speech Signal Process. ASSP-38 (August 1990) 1446–1456.
[23] A.K. Soman, P.P. Vaidyanathan, T.Q. Nguyen, Linear phase paraunitary filter banks: theory, factorizations and applications, IEEE Trans. Signal Process. SP-41 (May 1993) 3480–3496.
[24] P. Vary, G. Wackersreuther, A unified approach to digital polyphase filter banks, Arch. E1. Übertr. (AEÜ) 37 (1/2) (1983) 29–34.
[25] J. Woods, S. O'Neil, Subband coding of images, IEEE Trans. Acoust. Speech Signal Process. ASSP-34 (October 1986) 1278–1288.
[26] E. Zwicker, H. Fastl, Psychoacoustics, Springer, Berlin, 1990.